

Inhibition of the Long non-coding RNA ZFAS1 attenuates pathogenic ferroptosis by sponging miR-150-5p to activate CCND2 against diabetic cardiomyopathy

Tingjuan Ni

Wenzhou Medical College First Affiliated Hospital: The First Affiliated Hospital of Wenzhou Medical University

Xiaorong Chen

Wenzhou Medical University First Affiliated Hospital: The First Affiliated Hospital of Wenzhou Medical University

Xingxiao Huang

Zhejiang University - Zijiangang Campus: Zhejiang University

Sunlei Pan

Wenzhou Medical College First Affiliated Hospital: The First Affiliated Hospital of Wenzhou Medical University

Zhongqiu Lu (✉ lzq_640815@163.com)

the First Affiliated Hospital, Wenzhou Medical University

Original investigation

Keywords: Diabetic cardiomyopathy, lncRNA-ZFAS1, Ferroptosis, miR-150-5p, CCND2

Posted Date: January 15th, 2021

DOI: <https://doi.org/10.21203/rs.3.rs-144450/v1>

License:   This work is licensed under a Creative Commons Attribution 4.0 International License.

[Read Full License](#)

Abstract

Background

Diabetic cardiomyopathy (DCM) needs to be responsible for the increasing morbidity and mortality in diabetic patients with heart failure. Unfortunately, the pathogenesis of DCM has yet to be elaborate. Here we investigate the important role of lncRNA-ZFAS1 in the pathological process of DCM associated with ferroptosis.

Methods

Microarray data analysis of DCM in the patients or mice model from GEO was presented that ZFAS1 was significantly upregulated, miR-150-5p and CCND2 were significantly downregulated. High glucose (HG)-treated cardiomyocytes and db/db mice were simulated DCM *in vitro* and *in vivo*. Ad-ZFAS1, Ad-sh-ZFAS1, mimic miR-150-5p, Ad-CCND2, Ad-sh-CCND2 were injected into mice model or transfected into HG-treated Cardiomyocytes to clarify whether ZFAS1 can regulate miR-150-5p and CCND2 on ferroptosis. Effect of ZFAS1 on the left ventricular myocardial tissues in db/db mice and HG-treated cardiomyocytes, ferroptosis and apoptosis was determined by Masson staining, immunohistochemical staining, western blot, MBB staining, immunofluorescence staining and JC-1 staining. The relationship among ZFAS1, miR-150-5p, CCND2 was identified by dual luciferase reporter assay and RNA Pull-down assay.

Results

Inhibition of ZFAS1 led to the reduced collagen deposition, decreased cardiomyocytes apoptosis, ferroptosis and attenuated the DCM progress. ZFAS1 can sponge miR-150-5p to regulate CCND2 expression. Ad-sh-ZFAS1, miR-150-5p mimic and Ad-CCND2 transfection contributed to attenuate ferroptosis and DCM both *in vitro* and *in vivo*, while transfection Ad-ZFAS1 could reverse the positive effect of miR-150-5p mimic and Ad-CCND2 both *in vitro* and *in vivo*.

Conclusion

lncRNA-ZFAS1 acted as a ceRNA to sponge miR-150-5p can regulate CCND2 to promote cardiomyocytes ferroptosis and developed DCM, and inhibition of ZFAS1 could be a promising therapeutic target for the treatment and prevention of DCM.

Introduction

Diabetes makes patients vulnerable to a series of cardiovascular complications, one of the most serious progress is associated with the heart failure [1, 2]. With the increasing of the incidence of diabetes (expected to reach 693 million by 2045 [3]), heart failure caused by diabetes has become a worldwide

epidemic [4, 5]. Indeed, diabetes accounts for 1/3 of patients with heart failure in clinical, and diabetes has always been an independent predictor of adverse outcomes [6]. Instead, DCM is currently recognized as a proximate cause of heart failure with a 4-5fold increase in the risk of heart failure among diabetic patients which firstly described by the Framingham Heart Study 5 decades ago [2, 7, 8]. Despite the extensive research attention in diabetic cardiomyopathy recently [9], however, the full spectrum of possible pathogenesis and their relative contribution to the heart failure phenotype in diabetes are still incompletely understood.

The long noncoding ribonucleic acids (lncRNAs), non-coding RNA longer than 200 nucleotides in length, which participate in multiple biological processes, including cell metabolism, cell proliferation, cell fate determination, cell apoptosis and cell death, result in a variety of pathological conditions, such as cancer, Alzheimer's disease, emerge evidence has shown that lncRNAs regulated cardiac diseases [10–13]. Cardiac-related lncRNA-ZFAS1 (zinc finger antisense 1) was proved to associate with acute myocardial infarction [14–17]. Nevertheless, the mechanism between lncRNA-ZFAS1 with diabetic cardiomyopathy is still lacking.

One of lncRNAs' significant function was action as competing endogenous RNAs (ceRNAs) to sponge macromolecules, such as micro-RNAs (miRNAs) and proteins [18], which associated with a range of physiological, biological and pathological processes, including cardiac diseases [19, 20]. A clinical research demonstrated that miR-150-5p was significantly reduced in patients with heart failure, and represented an independent predictor of heart failure [21]. Furthermore, miR-150-5p could mitigate apoptosis in sepsis-induced myocardial depression [22], alleviate the progression of myocardial fibrosis [23], rescue cardiomyocytes from hypoxia-induced injury under the command of lncRNAs FOXD3-AS1 [24]. However, the role of miR-150-5p in diabetic cardiomyopathy and the relation with lncRNA-ZFAS1 have not been studied. Cyclin D2 (CCND2) could regulate the proliferation of cardiac myocytes [25], and is beneficial to the cardiac dysfunction [26], activates cell-cycle progression to enhance myocardial repair [27]. However, the role of CCND2 in diabetic cardiomyopathy have not been studied.

Ferroptosis, an iron-dependent regulated necrosis associated with a new form of regulatory cell death firstly described in 2012 [28], which could induce the pathological process of cancer, stroke, cardiovascular disease, and kidney failure [29, 30]. Glutathione peroxidase 4 (GPX4) could terminated the process of ferroptosis which involved in caspase and necrosomal complex [31]. Recent report has demonstrated that inhibiting ferroptosis could decrease mitochondrial iron to alleviate DOX-induced cardiac injury [32], but its role in diabetic cardiomyopathy remains to be explored.

In this study, we used HG-treated cardiomyocytes and db/db mice to simulate DCM *in vitro* and *in vivo* and investigated the identification of lncRNA-ZFAS1, which is upregulated during DCM, and show that inhibition of ZFAS1 alleviate the development of DCM by reducing ferroptosis via stabilizing miR-150-5p to activate CCND2.

Research Design And Methods

Ethics and Animal Experiments

The Institutes of the First Affiliated Hospital of Wenzhou Medical University Health Guidelines on the Use of Laboratory Animals to guide for the humanitarian care of animals.

Male db/+ mice and db/db mice (7 weeks old, weight 24 g) were fed a normal diet for four weeks under a 14-hour light / 8-hour dark cycle at 24 °C which purchased from the Model Animal Research Center of Nanjing University (Nanjing, China). The equal volume adenovirus (Ad-ZFAS1, Ad-sh-ZFAS1, Ad-CCND2, Ad-sh-CCND2) were injected into the left ventricle free wall of mice (40 μ L respectively, 10 μ L for each of four sites). MiR-150-5p mimics and mimic control (NC) were injected into the tail vein of mice (50 μ g/kg) for every 15 days for 12 weeks. Each group contains 8 mice.

Primary Culture of Neonatal Cardiomyocytes and Cell Transfection

Primary cardiomyocytes were isolated from the newborn (1- to 2-day-old) mice according to the professional article [33]. Cardiomyocytes were transfected with the adenovirus including Ad-ZFAS1, Ad-sh-ZFAS1, Ad-CCND2, Ad-sh-CCND2 (10 μ L/mL, MOI: 100:1, the titer of the adenoviruses was approximately 1.2×10^{10} PFU/mL, Hanbio Technology Ltd. Shanghai, China) in serum-free Dulbecco's Modified Eagle Medium (DMEM) for 6–8 h, the miR-150-5p mimics and mimic control (NC) (Sigma, St. Louis, MO, USA) were transfected into cardiomyocytes using Lipofectamine® 3000 (Invitrogen; Carlsbad, CA, USA), and then cultured in absence or presence of high glucose (HG, 25 mmol/L glucose).

Microarray-Based Gene Expression Data Analysis

The microarray data of diabetic and non-diabetic patients affected by heart failure (HF) based on the GSE26887, the micro-RNAs in pathophysiology of diabetic cardiomyopathy based on the GSE44179, the expression data from Rat ventricles 3 days, 28 days, and 42 days after STZ injection base on GSE4745, were acquired from the Gene Expression Omnibus (GEO) database (<https://www.ncbi.nlm.nih.gov/geo/>), differentially DCM-related genes were screened by Excel (Microsoft) with the threshold of $|\log_2FC| > 2.0$ and adj.P.Val (P value after correction) < 0.05 .

Dual luciferase reporter assay

The online database StarBase v2.0 predicted the binding site of miR-150-5p with lncRNA-ZFAS1 (<http://starbase.sysu.edu.cn/agoClipRNA.php?source=lncRNA>). MiR-150-5p was predicted to binding with CCND2 by online database TargetScan software (http://www.targetscan.org/mamm_31/). Wide sequences (wt-ZFAS1 and wt-CCND2) and mutant sequences (mut-ZFAS1 and mut-CCND2) were designed and synthesized according to the predicted binding sites. The human embryonic kidney cell line (HEK293T cells, ATCC, Manassas, VA) were cultured in 24-well plates reached to 80% confluence, the miR-150-5p mimic (30 n M) or miR-138-5p mimic negative controls (30 n M, Gene-Pharma, Shanghai, China) using Lipofectamine 3000 reagent (Thermo Fisher Scientific, USA) to co-transfected into HEK293T cells.

After 48 hours, the luciferase activity was explored by the Dual-Luciferase Reporter Assay Kit (Promega, USA).

Quantitative real time PCR (qRT-PCR)

The expression of ZFAS1, CCND2 and miR-150-5p were measured by qRT-PCR. Total RNA in left ventricle tissue and cardiomyocytes was extracted using the TRIzol reagent (Invitrogen) and RNA extraction kit (TaKaRa), miRNA was extracted using the miRNeasy Mini Kit (Qiagen, Germany) from the total RNA. RT-qPCR was performed according to the manufacturer's protocol on a QuantStudio 5 Real-Time PCR System (Thermo Fisher Scientific, USA). The primer sequences were listed as below: ZFAS1 (forward: 5'-ACGTGCAGACATCTACAAC CT-3' and reverse: 5'-TACTTCCAACACCCGCAT-3'), miR-150-5p, forward: 5'-TCGG CGTC TCCC AACC CTTG TAC-3', reverse: 5'-GTCG TATC CAGT GCAG GGTC CGAG GT-3', CCND2 (forward: 5'-AGAGCCACCGGTATGGAGCTGCTGTGCCACGAGGT 3', reverse: 5'-CTGCAGGCGCGCCGAATTTTTTTTTTAAGTTTCACCCT 3').

RNA pull-down assay

Biotinylated wild-type miR-150-5p (Bio-wt-150-5p) or biotinylated mutant miR-150-5p (Bio-mut-150-5p) or biotinylated miRNA which not complementary to ZFAS1 (Bio-NC) were transfected into primary cardiomyocytes. Forty-eight hours after transfection, cardiomyocytes were obtained for biotin-based pull-down assay (Thermo Fisher Scientific, USA) according to the protocol. ZFAS1 expression levels were measured by real-time PCR.

Magnetic bead coated by a ZFAS1 probe or a random probe were added into cardiomyocytes lysate. MiR-150-5p was eluted from the streptavidin beads after washing and enrichment of beads/RNA complex. MiR-150-5p expression level was measured by Northern Blot (Thermo Fisher Scientific, USA) according to the protocol.

Cell immunofluorescence staining

After fixed with 4% paraformaldehyde for 15 minutes, permeabilized with 0.5% Triton X-100 for 20 minutes, and blocked with 4% goat serum for 30 minutes at 37 °C, the adherent experimental cardiomyocytes were cultured with the primary antibody against Ferritin Heavy Chain (ab65080) at 4 °C overnight. Next day, after incubated with DyLight 488 and 594 AffiniPure Goat IgG (H + L) for 1 h at 37 °C and counterstained with 0.1 µg/mL DAPI (P36941; Invitrogen) for 3 minutes, images were measured by a Nikon Eclipse Ti-U fluorescence microscope.

Histology and immunohistochemistry

After dewaxed in 60 °C incubator, hydrated with xylene and anhydrous ethanol, antigen repaired with Citrate Antigen Retrieval Solution Sections (Beyotime, China) Sections (5-mm thickness) of the left ventricular myocardial tissues were incubated with primary antibodies against Ferritin Heavy Chain (FTH1, ab65080), 4-Hydroxynonenal (4-HNE, ab46545) at 4 °C overnight. Next day, sections were incubated with secondary antibodies at 37 °C for 30 minutes and then stained with 3,3'-Diaminobenzidine

(Gene Tech, China) at 37 °C for 5 minutes, photographed immediately in the dark using Nikon Eclipse Ti-U fluorescence microscope (Tokyo, Japan).

Masson staining

Masson staining was used to measure cardiac collagen content. After dewaxed in 60 °C incubator, hydrated with xylene and anhydrous ethanol, dyed with hematoxylin and Lichun red acid, Sections (5-mm thickness) of the left ventricular myocardial tissues were finally dyed with 1% phosphomolybdic acid, photographed immediately in the dark using Nikon Eclipse Ti-U fluorescence microscope (Tokyo, Japan). Collagen fibers were blue (aniline blue) or green (bright green), muscle fibers and cellulose were red.

Monobromobimane (MBB) staining

MBB staining was used to determine the glutathione (GSH) in cardiomyocytes. Cardiomyocytes were stained by MBB (20 µM; Sigma-Aldrich, USA) in PBS for 15 minutes at 37 °C, photographed immediately in the dark using Nikon Eclipse Ti-U fluorescence microscope (Tokyo, Japan).

JC-1 staining

JC-1 staining was used to determine the mitochondrial membrane potential. Cardiomyocytes were stained with JC-1 (MCE, NJ, USA) in PBS for 30 min at 37 °C, photographed immediately in the dark using Nikon Eclipse Ti-U fluorescence microscope (Tokyo, Japan).

Western blotting

Left ventricle tissue and cardiomyocytes were lysed to extract protein which separated by SDS-PAGE and then transferred onto 0.45 µm polyvinylidene difluoride transfer membranes (PVDF, Millipore, USA). After blocked and incubated with the primary antibodies, including GPX4 (ab125066), CCND2 (ab207604), cleaved caspase 3 (ab13847), Bcl-2 (ab32124), Bax (ab53154), and β-actin (ab8226) overnight at 4 °C, PVDF membranes were incubated with a peroxidase-conjugated secondary antibody, including anti-mouse and anti-rabbit (Abbkine, Redlands, CA), finally visualized using an ECL Plus Detection Reagent (Sigma, United States).

Statistical analysis

SPSS version 26.0 software (SPSS Inc, USA, IL) was used to analysis data which shown as mean ± standard deviation (SD) and perform Student's t test and ANOVA to show differences between two groups or multiple groups. All experiments were repeated at least three times and p values less than 0.05 were considered significant.

Results

Upregulated ZFAS1 expression and increased ferroptosis involved in diabetic cardiomyopathy and HG-treated cardiomyocytes.

The differentially HF-related genes profiles in diabetic patients and non-diabetic patients were screened out from the GSE26887 in the GEO database, lncRNA-ZFAS1 was significantly upregulated in the diabetic patients with HF (Fig. 1A). To determine whether ZFAS1 was really involved in diabetic cardiomyopathy, the expression of ZFAS1 in the left ventricular myocardial tissues of db/db mice and HG-treated cardiomyocytes was determined by RT-qPCR. The result revealed that ZFAS1 was significantly upregulated at the same way (Fig. 1B-C).

As shown in Fig. 1D, FTH1, a key iron storage protein involved in iron metabolism and act as ferritinophagy biomarkers, was decreased in the left ventricular myocardial tissues of db/db mice evaluated by immunohistochemical staining (Fig. 1D). 4-hydroxynonenal (4-HNE), the final product of lipid hydroperoxidation, was increased in the left ventricular myocardial tissues of db/db mice evaluated by immunohistochemical staining (Fig. 1D). Glutathione peroxidase 4 (GPX4), which could terminate the process of ferroptosis, was decreased in the left ventricular myocardial tissues of db/db mice measured by western blot (Fig. 1E-F). In keeping with *in vivo* results, FTH1 was seen colocalized rarely in the cytoplasm in HG-treated cardiomyocytes (Fig. 1G). We also observed a reduction in the expression of GPX4 in HG-treated cardiomyocytes measured by western blot (Fig. 1H-I). Taking together, we found that the expression of ZFAS1 was upregulated and ferroptosis was increased in diabetic cardiomyopathy and HG-treated cardiomyocytes.

Inhibition of ZFAS1 repressed ferroptosis in diabetic cardiomyopathy and HG-Treated Cardiomyocytes.

To further identify the function of ZFAS1 in the process of DCM, we injected Ad-ZFAS1, Ad-sh-ZFAS1 into the left ventricle free wall of mice. Masson staining showed a significant decrease of collagen deposition in the left ventricular myocardial tissues of db/db + Ad-ZFAS1 group (Fig. 2A). Inhibition of ZFAS1 could restore the expression of FTH1, reduce the expression of 4-HNE evaluated by immunohistochemical staining (Fig. 2B), rescue the expression of GPX4 and inhibit the expression of apoptosis-related genes including Cleaved caspase 3, Bax, and Bcl-2 measured by western blot (Fig. 2C-D). Inhibition of ZFAS1 in HG-treated cardiomyocytes could increase intracellular GSH levels assessed by MBB staining to a certain extent (Fig. 2E), restore the distribution of FTH1 in the cytoplasm (Fig. 2F), alleviate the mitochondrial membrane potential as revealed by the transition from red fluorescence to green fluorescence measured by JC-1 staining (Fig. 2G), rescue the expression of GPX4 and inhibit the expression of apoptosis-related genes including Cleaved caspase 3, Bax, and Bcl-2 measured by western blot (Fig. 2H-I). Altogether, these results suggested that inhibition of ZFAS1 could prevent ferroptosis from diabetic cardiomyopathy and HG-treated cardiomyocytes.

lncRNA-ZFAS1 can bind with miR-150-5p to regulate expression of CCND2.

The differentially role of micro-RNAs profiles pathophysiology of diabetic cardiomyopathy were screened out from the GSE44179 in the GEO database, we found that miR-150-5p was substantial reduced (Fig. 3A). To determine whether miR-150-5p was really involved in diabetic cardiomyopathy, the expression of miR-150-5p in the left ventricular myocardial tissues of db/db mice and HG-treated

cardiomyocytes was determined by RT-qPCR. The result revealed that miR-150-5p was significantly downregulated at the same way (Fig. 3B-C).

To elucidate the potential molecular mechanism by which ZFAS1 and miR-150-5p regulated DM, we attempted to explore the underlying target bind site between ZFAS1 and miR-150-5p. The predicted bind site of miR-150-5p and ZFAS1 was displayed in the Fig. 3D analyzed by bioinformatic program TargetScan. Dual luciferase reporter assay demonstrated that transfection with miR-150-5p mimics significantly reduced the relative firefly luciferase activity of wt-ZFAS1 whereas the mut-ZFAS1 luciferase activity was not affected (Fig. 3E). Further, we compared the sequences of ZFAS1 with that of miR-150-5p analyzed by the bioinformatics program RNAhybrid and investigated that ZFAS1 contains a binding site of miR-150-5p (Fig. 3F). What's more, we performed a biotin-avidin pull-down assay to explore whether miR-150-5p could directly bind to ZFAS1. ZFAS1 was pulled down by biotinylated wild-type miR-150-5p, the inability of miR-150-5p to pull down ZFAS1 when introduction of miR-150-5p mutations that destroy base pairing between ZFAS1 and miR-150-5p, indicating that the identification of miR-150-5p to ZFAS1 is sequence specific (Fig. 3G). We also performed inverse pull-down assay to test if ZFAS1 could pull-down miR-150-5p, the results showed that miR-150-5p could be co-precipitated by ZFAS1 using a biotin-labeled-specific ZFAS1 probe (Fig. 3H).

The GSE44179 from GEO database presented us that CCND2 was significantly decreased in rat ventricles after STZ injection (Fig. 3I). To determine whether CCND2 was really involved in diabetic cardiomyopathy, the expression of CCND2 in the left ventricular myocardial tissues of db/db mice and HG-treated cardiomyocytes was determined by western blot. The result revealed that CCND2 was significantly downregulated in the same way (Fig. 3J-M). The bioinformatic program TargetScan provided information for the predicted binding site of miR-150-5p and CCND2 (Fig. 3N). Additionally, the dual-luciferase reporter assay demonstrated that transfection with miR-150-5p mimics significantly reduced the relative firefly luciferase activity of wt-CCND2 whereas the mut-CCND2 luciferase activity was not affected (Fig. 3O). These results supported that ZFAS1 can bind with miR-150-5p to regulate the expression of CCND2.

ZFAS1 promoted ferroptosis in diabetic cardiomyopathy and HG-treated Cardiomyocytes through modulating miR-150-5p.

Because of the interaction between ZFAS1 and miR-150-5p, we further explored whether ZFAS1 was able to regulate ferroptosis through miR-150-5p. As shown in Fig. 4A, stimulation of miR-150-5p significantly decreased collagen deposition in the left ventricular myocardial tissues of db/db mice which was similar to the function of ZFAS1 inhibition. However, stimulation of ZFAS1 definitely abolished the positive effect of miR-150-5p detected by Masson staining. Overexpression of miR-150-5p could restore the expression of FTH1, reduce the expression of 4-HNE evaluated by immunohistochemical staining as the function of inhibition of ZFAS1, whereas overexpression of ZFAS1 offset the positive effect of miR-150-5p (Fig. 4B). Overexpression of miR-150-5p could rescue the expression of GPX4 and CCND2 and inhibit the expression of apoptosis-related genes including Cleaved caspase 3, Bax, and Bcl-2 measured by western

blot which were similar to the function of ZFAS1, whereas overexpression of ZFAS1 counteracted the positive effect of miR-150-5p (Fig. 4C-D).

Subsequently, we explored whether ZFAS1 regulate ferroptosis through miR-150-5p in HG-treated cardiomyocytes. As shown in Fig. 4E, HG-treated cardiomyocytes transfected with Ad-sh-ZFAS1 or mimic miR-150-5p all made sense in the increase of intracellular GSH levels assessed by MBB staining (Fig. 4E), whereas overexpression of ZFAS1 counteracted the positive effect of miR-150-5p. Moreover, Ad-ZFAS1 administration significantly reversed the effect of miR-150-5p, as demonstrated by a reduction in the expression of FTH1 as detected via immunofluorescence (Fig. 4F), the decrease in mitochondrial membrane potential as detected via JC-1 staining (Fig. 4G), a reduction in the expression of GPX4 and CCND2 and a reduction in the expression of apoptosis-related genes including Cleaved caspase 3, Bax, and Bcl-2 measured by western blot (Fig. 4H-I).

Taking together, these results indicated that inhibition of ZFAS1 could suppress ferroptosis in diabetic cardiomyopathy and HG-treated Cardiomyocytes through targeting miR-150-5p. lncRNA-ZFAS1 acted as a ceRNA to sponge miR-150-5p.

ZFAS1 promoted ferroptosis in diabetic cardiomyopathy and HG-treated Cardiomyocytes through modulating CCND2.

To further elucidate the role of CCND2 in the positive function of ZFAS1 inhibition against ferroptosis in diabetic cardiomyopathy and HG-treated Cardiomyocytes, the left ventricular myocardial tissues of db/db mice were injected with Ad-sh-ZFAS1, Ad-ZFAS1, Ad-CCND2, or Ad-sh-CCND2. Interestingly, overexpression of CCND2 exerted a marked effect in inhibition of ferroptosis likewise the function as the inhibition of ZFAS1, however, these effects were eliminated when stimulation of ZFAS1 corroborated by the increased collagen deposition measured by Masson staining (Fig. 5A), the decreased expression of FTH1 and increased the expression of 4-HNE measured by immunohistochemical staining (Fig. 5B), the decreased expression of GPX4 and the increased expression of apoptosis-related genes including Cleaved caspase 3, Bax, and Bcl-2 measured by western blot (Fig. 5C-D) in the left ventricular myocardial tissues of db/db mice, the decreased of intracellular GSH levels assessed by MBB staining (Fig. 5E), the reduction expression of FTH1 as detected via immunofluorescence (Fig. 5F), the decreased mitochondrial membrane potential as detected via JC-1 staining (Fig. 5G), the reduction in the expression of GPX4 and the reduction in the expression of apoptosis-related genes including Cleaved caspase 3, Bax, and Bcl-2 measured by western blot (Fig. 5H-I). Cumulatively, these results demonstrated that ZFAS1 inhibition suppressed ferroptosis in diabetic cardiomyopathy and HG-treated Cardiomyocytes through modulating CCND2. lncRNA-ZFAS1 acted as a ceRNA to sponge miR-150-5p can regulate CCND2.

Discussion

Diabetes mellitus is an independent risk of heart failure (HF), while HF could accelerate diabetes mellitus cardiovascular complication [5], according to a report, 15%-35% of HF patients should be blamed to diabetic patients [34]. What's more, diabetic cardiomyopathy is considered an indispensable pathophysiological

state among diabetic patients which could result in the dysfunctional cardiomyocytes, abnormal myocardial and the final cardiac dysfunction characterized by left ventricular longitudinal dysfunction [8, 35, 36]. However, the therapy or specific treatment of DCM in clinical is a considerable challenge. To date, there is still no identified molecular mechanism of DCM to guide the treatment of DCM. In the present study, we aimed to elucidate the role of lncRNA-ZFAS1, miR-150-5p, CCND2 in ferroptosis of cardiomyocytes in DCM. Specifically, inhibition of ZFAS1 could potentially alleviate myocardial fibrosis in DCM by inhibiting cardiomyocyte ferroptosis via sponging miR-150-5p to activate CCND2.

These decade, the roles of lncRNAs were paid attention to various cardiovascular diseases, especially myocardial infarction (MI) [20, 37–39], but little is known about the role of lncRNAs in the pathogenesis of DCM. The GSE26887 from GEO database show that lncRNA-ZFAS1 was significantly upregulated in diabetic patients with HF, compared with non-diabetic patients (Fig. 1A). As we expected, ZFAS1 was also upregulated in diabetic cardiomyopathy and HG-treated cardiomyocytes (Fig. 1B-C). ZFAS1 is one of cardiac-related lncRNAs, previously, knockdown of lncRNA-ZFAS1 prevents cardiomyocytes from MI [14]. Reports emphasized that ZFAS1 was upregulated to promote cardiac disease [40] and induce mitochondria-mediated cardiomyocytes apoptosis [16].

Ferroptosis, a unique cell death, characterized by the stimulation of reactive oxygen species (ROS) result in the mitochondria dysfunction induced by iron catalytic activity and lipid peroxidation [41]. Growing studies has shown that ferroptosis was also a critical form of cardiomyocytes death [42, 43]. In this study, we found that ferroptosis was accumulated in the left ventricular myocardial tissues of DCM and HG-treated cardiomyocytes, as demonstrated by the downregulation expression of iron storage protein FTH1 as determined by immunohistochemical staining (Fig. 1D) and immunofluorescence staining (Fig. 1G), the upregulation expression of the final product of lipid hydroperoxidation protein 4-HNE as determined by immunohistochemical staining (Fig. 1D), the downregulation expression of the ferroptosis termination protein GPX4 determined by western blot analysis (Fig. 1E-F, 1H-I).

Moreover, we found that the inhibition of ZFAS1 in db/db mice could attenuate ferroptosis in the left ventricular myocardial tissues of DCM and HG-treated cardiomyocytes based on the upregulation expression of FTH1 as determined by immunohistochemical staining (Fig. 2B) and immunofluorescence staining (Fig. 2F), the upregulation expression of the ferroptosis termination protein GPX4 as determined by western blot analysis (Fig. 2C-D, 2-H-I), the increased intracellular GSH levels assessed by MBB staining (Fig. 2E), the restoration of mitochondrial membrane potential measured by JC-1 staining, all the change related with ferroptosis resulted in the reduction of the collagen deposition to attenuate cardiac fibrosis in myocardial tissue as determined by Masson staining (Fig. 2A) and the decreased expression of apoptosis-related genes including Cleaved caspase 3, Bax, and Bcl-2 measured by western blot (Fig. 2C-D, 2-H-I).

Emerging evidence has shown that miR-150-5p involved in heart disease and HF [44, 45]. The GSE44179 from GEO database and the RT-qPCR of left ventricular myocardial tissues of db/db mice and HG-treated cardiomyocytes all show that miR-150-5p was significantly downregulated (Fig. 3A-C). Type D cyclins

regulate the transition of cell cycle from G1 to S, while overexpression of CCND2 (cyclin D2) can activate the cell cycle of cardiomyocytes [25, 46]. The GSE4745 from GEO database and the RT-qPCR of left ventricular myocardial tissues of db/db mice and HG-treated cardiomyocytes all show that CCND2 was significantly downregulated (Fig. 3I-M). Further, we identified that ZFAS1 can bind with miR-150-5p to regulate expression of CCND2 as determined by RNA Pull-down assay (Fig. 3G-H), dual luciferase reporter assay (Fig. 3E, O), RNAhybrid program (Fig. 3F) and TargetScan program (Fig. 3D, N).

More importantly, overexpression of miR-150-5p and CCND2 significantly alleviated ferroptosis which was similar to the function of ZFAS1 inhibition in db/db mice and HG-treated Cardiomyocytes, however, these positive effects were eliminated when stimulation of ZFAS1 based on the downregulation expression of FTH1 as determined by immunohistochemical staining (Fig. 4B, Fig. 5B) and immunofluorescence staining (Fig. 4F, Fig. 5F), the downregulation expression of the ferroptosis termination protein GPX4 as determined by western blot analysis (Fig. 4C-D and 4H-I, Fig. 5C-D and 5H-I), the decreased intracellular GSH levels assessed by MBB staining (Fig. 4E, Fig. 5E), the reduction of mitochondrial membrane potential measured by JC-1 staining (Fig. 4G, Fig. 5G), all the change related with ferroptosis resulted in the accumulation of the collagen deposition which induce cardiac fibrosis in myocardial tissue as determined by Masson staining (Fig. 4A, Fig. 5A) and the increased expression of apoptosis-related genes including Cleaved caspase 3, Bax, and Bcl-2 measured by western blot (Fig. 4C-D and 4H-I, Fig. 5C-D and 5H-I). Such findings strongly supported that inhibition of ZFAS1 could inhibit cardiomyocytes ferroptosis by sponging miR-150-5p to activate CCND2 against diabetic cardiomyopathy (Fig. 6).

Conclusion

Together, all these results strongly suggested that simulation of ZFAS1 indeed promote ferroptosis in DCM, lncRNA-ZFAS1 acted as a ceRNA to sponge miR-150-5p can regulate CCND2. Most important of all, inhibition of ZFAS1 could suppress cardiomyocytes ferroptosis and attenuated DCM progress. The ability to target lncRNA-ZFAS1 will pave the way for the novel treatment of DCM.

Abbreviations

DCM: Diabetic cardiomyopathy; HG: High glucose; lncRNAs: The long noncoding ribonucleic acids; ZFAS1: zinc finger antisense 1; ceRNAs: competing endogenous RNAs; miRNAs: micro-RNAs; GPX4: Glutathione peroxidase 4; GEO: Gene Expression Omnibus; FTH1: Ferritin Heavy Chain; 4-HNE: 4-Hydroxynonenal; GSH: glutathione; MBB: Monobromobimane.

Declarations

Ethics approval and consent to participate

The animal experiments were approved by the Institutes of the First Affiliated Hospital of Wenzhou Medical University Health Guidelines on the Use of Laboratory Animals.

Consent for publication

All authors have declared their Consent for this publication.

Availability of data and materials

All data and materials are available upon request.

Acknowledgements

None.

Authors' contributions

Tingjuan Ni and Zhiongqiu Lu designed the study. Tingjuan Ni, Xiaorong Chen, Xingxiao Huang, and Sunlei Pan carried out the in vitro and in vivo experiment. Tingjuan Ni and Xingxiao Huang analyzed the data. Tingjuan Ni and Xiaorong Chen designed the study and drafted the paper. All authors reviewed and approved the final manuscript.

Authors' information

¹ Department of Emergency Intensive Care Unit, the First Affiliated Hospital, Wenzhou Medical University, Wenzhou, Zhejiang, China. ² Department of Cardiology, Zhejiang University, Hangzhou, Zhejiang, China. ³ Department of Coronary Care Unit, the First Affiliated Hospital, Wenzhou Medical University, Wenzhou, Zhejiang, China.

Competing interests

The authors declare that they have no competing interests.

Funding

This study was supported by the National Natural Science Foundation of China (No. 81772112).

References

1. Ritchie RH, Abel ED: **Basic Mechanisms of Diabetic Heart Disease**. *CIRC RES* 2020, **126**(11):1501-1525.
2. Kannel WB, Hjortland M, Castelli WP: **Role of diabetes in congestive heart failure: The Framingham study**. *The American Journal of Cardiology* 1974, **34**(1):29-34.

3. Cho NH, Shaw JE, Karuranga S, Huang Y, Da Rocha Fernandes JD, Ohlrogge AW, Malanda B: **IDF Diabetes Atlas: Global estimates of diabetes prevalence for 2017 and projections for 2045.** *DIABETES RES CLIN PR* 2018, **138**:271-281.
4. Ni T, Lin N, Huang X, Lu W, Sun Z, Zhang J, Lin H, Chi J, Guo H: **Icariin Ameliorates Diabetic Cardiomyopathy Through Apelin/Sirt3 Signalling to Improve Mitochondrial Dysfunction.** *FRONT PHARMACOL* 2020, **11**.
5. Varinder Kaur Randhawa SD: **How Diabetes and Heart Failure Modulate Each Other and Condition Management.** *CAN J CARDIOL* 2020, **20**(S0828-282X):31115-31116.
6. Ohkuma T, Komorita Y, Peters SAE, Woodward M: **Diabetes as a risk factor for heart failure in women and men: a systematic review and meta-analysis of 47 cohorts including 12 million individuals.** *DIABETOLOGIA* 2019, **62**(9):1550-1560.
7. Leon BM: **Diabetes and cardiovascular disease: Epidemiology, biological mechanisms, treatment recommendations and future research.** *World Journal of Diabetes* 2015, **6**(13):1246.
8. Zamora M, Villena JA: **Contribution of Impaired Insulin Signaling to the Pathogenesis of Diabetic Cardiomyopathy.** *INT J MOL SCI* 2019, **20**(11).
9. Peterson LR, Gropler RJ: **Metabolic and Molecular Imaging of the Diabetic Cardiomyopathy.** *CIRC RES* 2020, **126**(11):1628-1645.
10. Kumarswamy R, Bauters C, Volkman I, Maury F, Fetisch J, Holzmann A, Lemesle G, de Groote P, Pinet F, Thum T: **Circulating Long Noncoding RNA, LIPCAR, Predicts Survival in Patients With Heart Failure.** *CIRC RES* 2014, **114**(10):1569-1575.
11. Uchida S, Dimmeler S: **Long Noncoding RNAs in Cardiovascular Diseases.** *CIRC RES* 2015, **116**(4):737-750.
12. Shah RV, Rong J, Larson MG, Yeri A, Ziegler O, Tanriverdi K, Murthy V, Liu X, Xiao C, Pico AR *et al*: **Associations of Circulating Extracellular RNAs With Myocardial Remodeling and Heart Failure.** *JAMA CARDIOL* 2018, **3**(9):871.
13. Zhang Y, Du W, Yang B: **Long non-coding RNAs as new regulators of cardiac electrophysiology and arrhythmias: Molecular mechanisms, therapeutic implications and challenges.** *PHARMACOL THERAPEUT* 2019, **203**:107389.
14. Wu T, Wu D, Wu Q, Zou B, Huang X, Cheng X, Wu Y, Hong K, Li P, Yang R *et al*: **Knockdown of Long Non-Coding RNA-ZFAS1 Protects Cardiomyocytes Against Acute Myocardial Infarction Via Anti-Apoptosis by Regulating miR-150/CRP.** *J CELL BIOCHEM* 2017, **118**(10):3281-3289.
15. Zhang Y, Jiao L, Sun L, Li Y, Gao Y, Xu C, Shao Y, Li M, Li C, Lu Y *et al*: **LncRNA ZFAS1 as a SERCA2a Inhibitor to Cause Intracellular Ca²⁺ Overload and Contractile Dysfunction in a Mouse Model of Myocardial Infarction.** *CIRC RES* 2018.
16. Jiao L, Li M, Shao Y, Zhang Y, Gong M, Yang X, Wang Y, Tan Z, Sun L, Xuan L *et al*: **lncRNA-ZFAS1 induces mitochondria-mediated apoptosis by causing cytosolic Ca²⁺ overload in myocardial infarction mice model.** *CELL DEATH DIS* 2019, **10**(12).

17. Wang J, Ruan J, Zhu M, Yang J, Du S, Xu P, Zhang Z, Wang P, Yang W, Yu M: **Predictive value of long noncoding RNA ZFAS1 in patients with ischemic stroke.** *CLIN EXP HYPERTENS* 2019, **41**(7):615-621.
18. Salmena L, Poliseno L, Tay Y, Kats L, Pandolfi PP: **A ceRNA hypothesis: the Rosetta Stone of a hidden RNA language?** *CELL* 2011, **146**(3):353-358.
19. Ong S, Katwadi K, Kwek X, Ismail NI, Chinda K, Ong S, Hausenloy DJ: **Non-coding RNAs as therapeutic targets for preventing myocardial ischemia-reperfusion injury.** *EXPERT OPIN THER TAR* 2018, **22**(3):247-261.
20. Niu X, Pu S, Ling C, Xu J, Wang J, Sun S, Yao Y, Zhang Z: **lncRNA Oip5-as1 attenuates myocardial ischaemia/reperfusion injury by sponging miR-29a to activate the SIRT1/AMPK/PGC1 α pathway.** *CELL PROLIFERAT* 2020, **53**(6).
21. Abu-Halima M, Meese E, Saleh MA, Keller A, Abdul-Khaliq H, Raedle-Hurst T: **Micro-RNA 150-5p predicts overt heart failure in patients with univentricular hearts.** *PLOS ONE* 2019, **14**(10):e223606.
22. Zhu XG, Zhang TN, Wen R, Liu CF: **Overexpression of miR-150-5p Alleviates Apoptosis in Sepsis-Induced Myocardial Depression.** *BIOMED RES INT* 2020, **2020**:1-10.
23. Shen J, Xing W, Gong F, Wang W, Yan Y, Zhang Y, Xie C, Fu S: **MiR-150-5p retards the progression of myocardial fibrosis by targeting EGR1.** *CELL CYCLE* 2019, **18**(12):1335-1348.
24. Zheng J, Peng B, Zhang Y, Ai F, Hu X: **FOXD3-AS1 Knockdown Suppresses Hypoxia-Induced Cardiomyocyte Injury by Increasing Cell Survival and Inhibiting Apoptosis via Upregulating Cardioprotective Molecule miR-150-5p In Vitro.** *FRONT PHARMACOL* 2020, **11**:1284.
25. BUSK P, HINRICHSSEN R, BARTKOVA J, HANSEN A, CHRISTOFFERSEN T, BARTEK J, HAUNSO S: **Cyclin D2 induces proliferation of cardiac myocytes and represses hypertrophy.** *EXP CELL RES* 2005, **304**(1):149-161.
26. Yamak A, Temsah R, Maharsy W, Caron S, Paradis P, Aries A, Nemer M: **Cyclin D2 rescues size and function of GATA4 haplo-insufficient hearts.** *AM J PHYSIOL-HEART C* 2012, **303**(8):H1057-H1066.
27. Zhu W, Zhao M, Mattapally S, Chen S, Zhang J: **CCND2 Overexpression Enhances the Regenerative Potency of Human Induced Pluripotent Stem Cell-Derived Cardiomyocytes.** *CIRC RES* 2018, **122**(1):88-96.
28. Dixon SJ, Lemberg KM, Lamprecht MR, Skouta R, Zaitsev EM, Gleason CE, Patel DN, Bauer AJ, Cantley AM, Yang WS *et al*: **Ferroptosis: an iron-dependent form of nonapoptotic cell death.** *CELL* 2012, **149**(5):1060-1072.
29. Paras K, Mishra AAJA: **Guidelines for evaluating myocardial cell death.** *AM J PHYSIOL-HEART C* 2019, **317**(5).
30. Hao Zhang PZSW: **Role of Iron metabolism in heart failure: From Iron deficiency to iron overload.** *BIOCHIMICA ET BIOPHYSICA ACTA-MOLECULAR BASIS OF DISEASE* 2018, **1865**(7):1925-1937.
31. Stockwell BR, Friedmann AJ, Bayir H, Bush AI, Conrad M, Dixon SJ, Fulda S, Gascon S, Hatzios SK, Kagan VE *et al*: **Ferroptosis: A Regulated Cell Death Nexus Linking Metabolism, Redox Biology, and Disease.** *CELL* 2017, **171**(2):273-285.

32. Fang X, Wang H, Han D, Xie E, Yang X, Wei J, Gu S, Gao F, Zhu N, Yin X *et al*: **Ferroptosis as a target for protection against cardiomyopathy**. *P NATL ACAD SCI USA* 2019, **116**(7):2672-2680.
33. Leone M, Engel FB: **Isolation, Culture, and Live-Cell Imaging of Primary Rat Cardiomyocytes**. *Methods Mol Biol* 2021, **2158**:109-124.
34. Cohen-Solal A, Beauvais F, Logeart D: **Heart Failure and Diabetes Mellitus: Epidemiology and Management of an Alarming Association**. *J CARD FAIL* 2008, **14**(7):615-625.
35. Dillmann WH: **Diabetic Cardiomyopathy**. *CIRC RES* 2019, **124**(8):1160-1162.
36. Tanaka H, Tatsumi K, Matsuzoe H, Matsumoto K, Hirata K: **Impact of diabetes mellitus on left ventricular longitudinal function of patients with non-ischemic dilated cardiomyopathy**. *CARDIOVASC DIABETOL* 2020, **19**(1).
37. Mao Q, Liang X, Zhang C, Pang Y, Lu Y: **LncRNA KLF3-AS1 in human mesenchymal stem cell-derived exosomes ameliorates pyroptosis of cardiomyocytes and myocardial infarction through miR-138-5p/Sirt1 axis**. *STEM CELL RES THER* 2019, **10**(1).
38. Sun L, Zhu W, Zhao P, Wang Q, Fan B, Zhu Y, Lu Y, Chen Q, Zhang J, Zhang F: **Long noncoding RNA UCA1 from hypoxia-conditioned hMSC-derived exosomes: a novel molecular target for cardioprotection through miR-873-5p/XIAP axis**. *CELL DEATH DIS* 2020, **11**(8):696.
39. Song Y, Wang B, Zhu X, Hu J, Sun J, Xuan J, Ge Z: **Human umbilical cord blood-derived MSCs exosome attenuate myocardial injury by inhibiting ferroptosis in acute myocardial infarction mice**. *CELL BIOL TOXICOL* 2020.
40. Tim Vervliet ELRH: **Lnc'ing Ca 2+ , SERCA and cardiac disease**. *CELL CALCIUM* 2018(72):132-134.
41. Wang Z, Chen X, Liu N, Shi Y, Liu Y, Ouyang L, Tam S, Xiao D, Liu S, Wen F *et al*: **A Nuclear Long Non-Coding RNA LINC00618 Accelerates Ferroptosis in a Manner Dependent upon Apoptosis**. *MOL THER* 2020.
42. Conrad M, Proneth B: **Broken hearts: Iron overload, ferroptosis and cardiomyopathy**. *CELL RES* 2019, **29**(4):263-264.
43. Baba Y, Higa JK, Shimada BK, Horiuchi KM, Suhara T, Kobayashi M, Woo JD, Aoyagi H, Marh KS, Kitaoka H *et al*: **Protective effects of the mechanistic target of rapamycin against excess iron and ferroptosis in cardiomyocytes**. *AM J PHYSIOL-HEART C* 2018, **314**(3):H659-H668.
44. Tianxiao Huan JRKT: **Dissecting the Roles of MicroRNAs in Coronary Heart Disease via Integrative GenomicDissecting the Roles of MicroRNAs in Coronary Heart Disease via Integrative GenomicAnalyses**. *Arterioscler Thromb Vasc Biol* 2015, **4**(35):1011-1021.
45. Domenico Scrutinio FCAP: **Circulating microRNA-150-5p as a novelbiomarker for advanced heart failure. A genome-wide prospective studymiR-150-5p in advancedheart failure**. *J Heart Lung Transplant* 2017, **6**(36):616-624.
46. Chengming Fan VGFY: **Cardiomyocytes from CCND2-overexpressing human induced-pluripotent stem cells repopulate the myocardial scar in mice: A6-month study**. 2019(137):25-33.

Figures

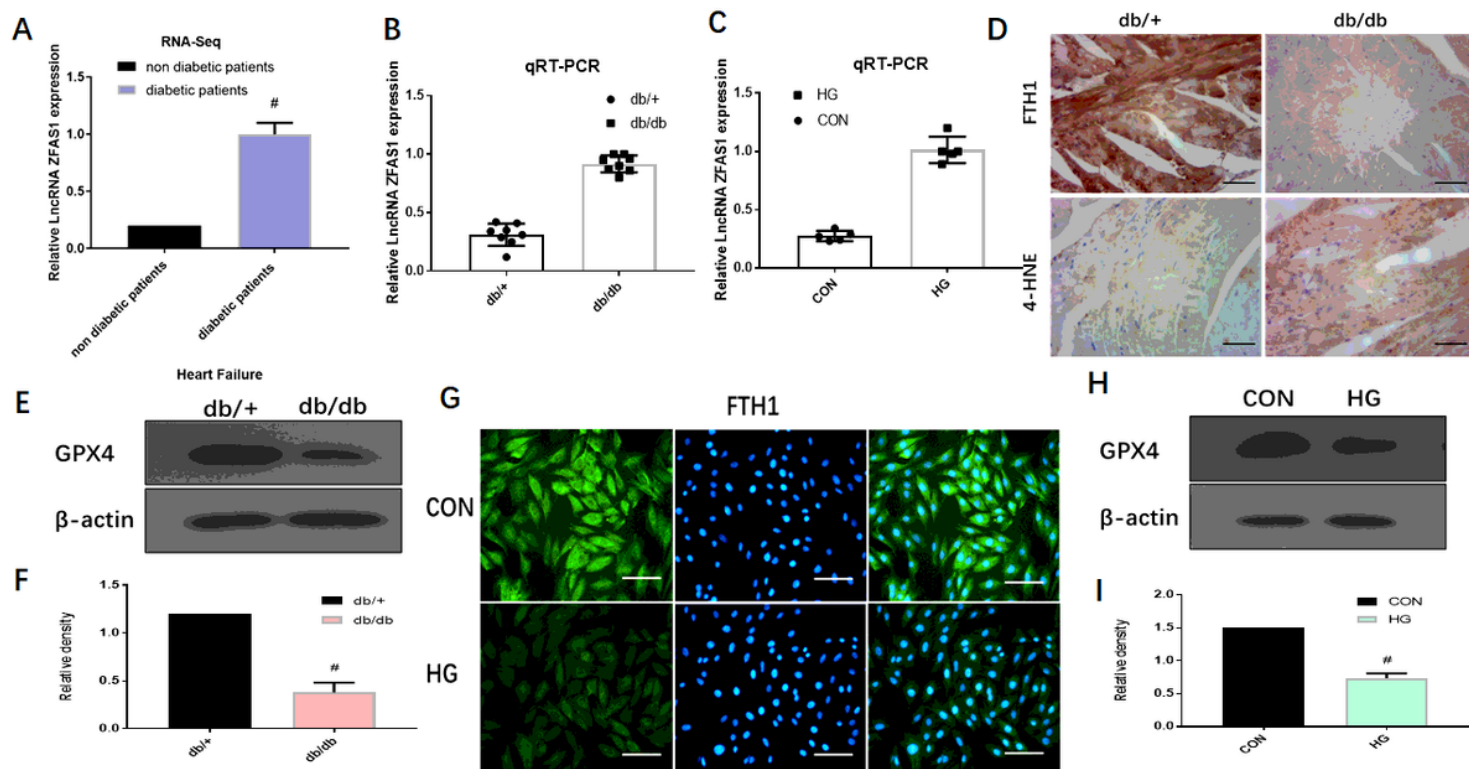


Figure 1

ZFAS1 is involved in the response to diabetic cardiomyopathy- and high glucose-induced ferroptosis. (A) ZFAS1 expression levels in heart failure of diabetic patients and non-diabetic patients from RNA-sequencing data (GSE26887). (B) RT-qPCR analysis of ZFAS1 expression in the left ventricular myocardial tissues of db/+ and db/db mice. (C) RT-qPCR analysis of ZFAS1 expression in control cardiomyocytes and HG-treated cardiomyocytes. (D) Relative expression of FTH1 and 4-HNE were determined by immunohistochemical staining in the left ventricular myocardial tissues of db/+ and db/db mice. (E-F) Relative protein expression of GPX4 was assessed by western blot analysis in the left ventricular myocardial tissues of db/+ and db/db mice. (G) Immunofluorescence against FTH1 (green) in control cardiomyocytes and HG-treated cardiomyocytes. (H-I) Relative protein expression of GPX4 was assessed by western blot analysis in control cardiomyocytes and HG-treated cardiomyocytes. # $P < 0.05$ vs CON group or db/+ group, data are measured as mean \pm SD (n=3).

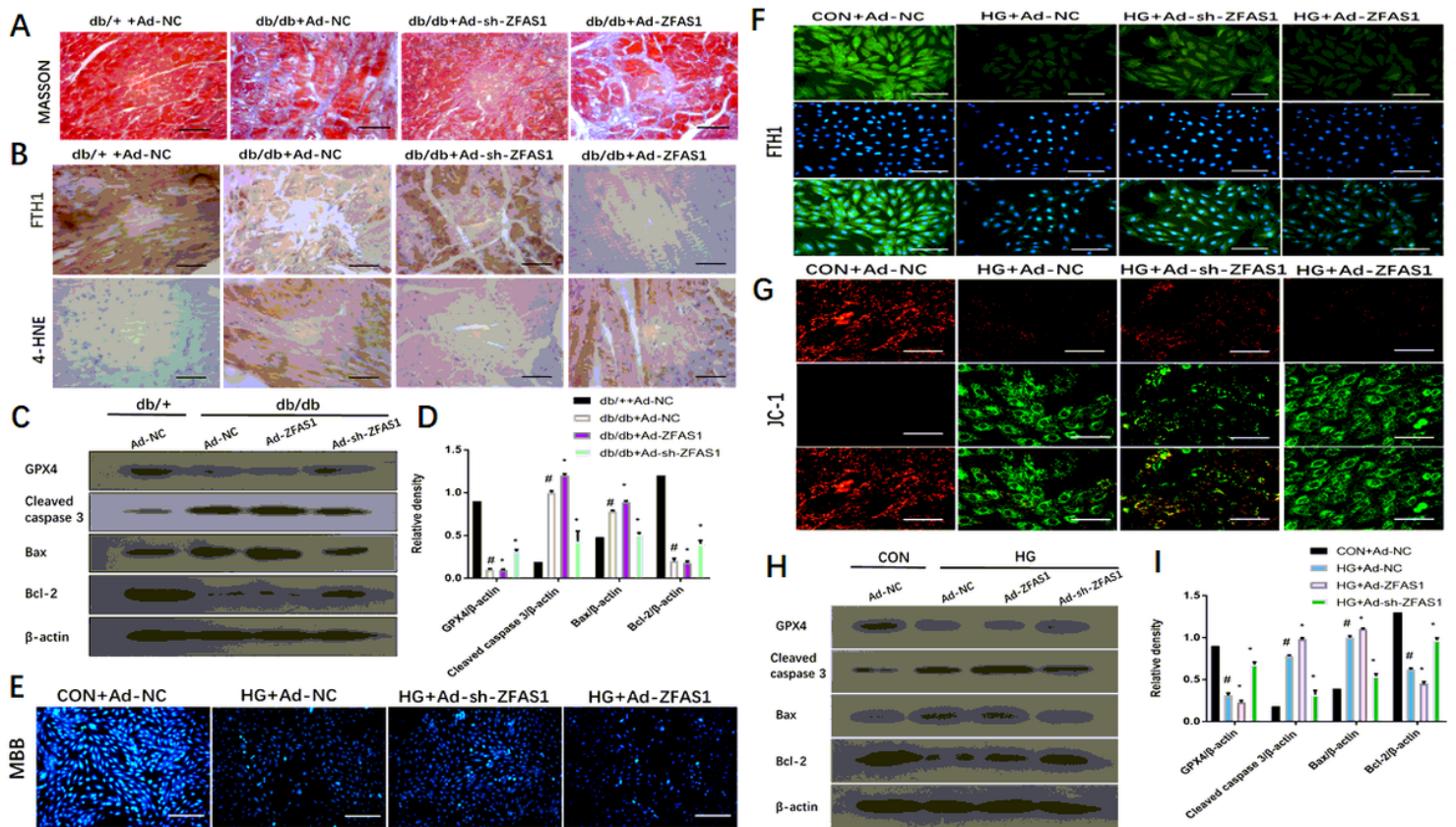


Figure 2

Inhibition of ZFAS1 alleviated ferroptosis induced in diabetic cardiomyopathy and HG-treated cardiomyocytes. Db/+mice (n = 8) and db/db mice (n=8) were injected with Ad-NC, Ad-ZFAS1, Ad-sh-ZFAS1, respectively. Cardiomyocytes were transfected with Ad-NC, Ad-ZFAS1, Ad-sh-ZFAS1 with or without under HG stimulation. (A) Masson staining was used to assess Collagen deposition in the left ventricular myocardial tissues in experimental mice (blue indicates collagen deposition). (B) Relative expression of FTH1 and 4-HNE were determined by immunohistochemical staining in the left ventricular myocardial tissues of experimental mice. (C-D) Relative protein expression of GPX4, Cleaved caspase 3, Bax, and Bcl-2 were assessed by western blot analysis in the left ventricular myocardial tissues of experimental mice. (E) MBB staining was used to assess GSH levels in experimental cardiomyocytes. (F) Immunofluorescence against FTH1 (green) in experimental cardiomyocytes. (G) JC-1 staining was used to assess mitochondrial membrane potential in experimental cardiomyocytes. (H-I) Relative protein expression of GPX4, Cleaved caspase 3, Bax, and Bcl-2 were assessed by western blot analysis in experimental cardiomyocytes. #P < 0.05 vs CON group or db/+ group, *P < 0.05 vs HG + Ad-NC or db/db + Ad-NC; data are measured as mean \pm SD (n=3).

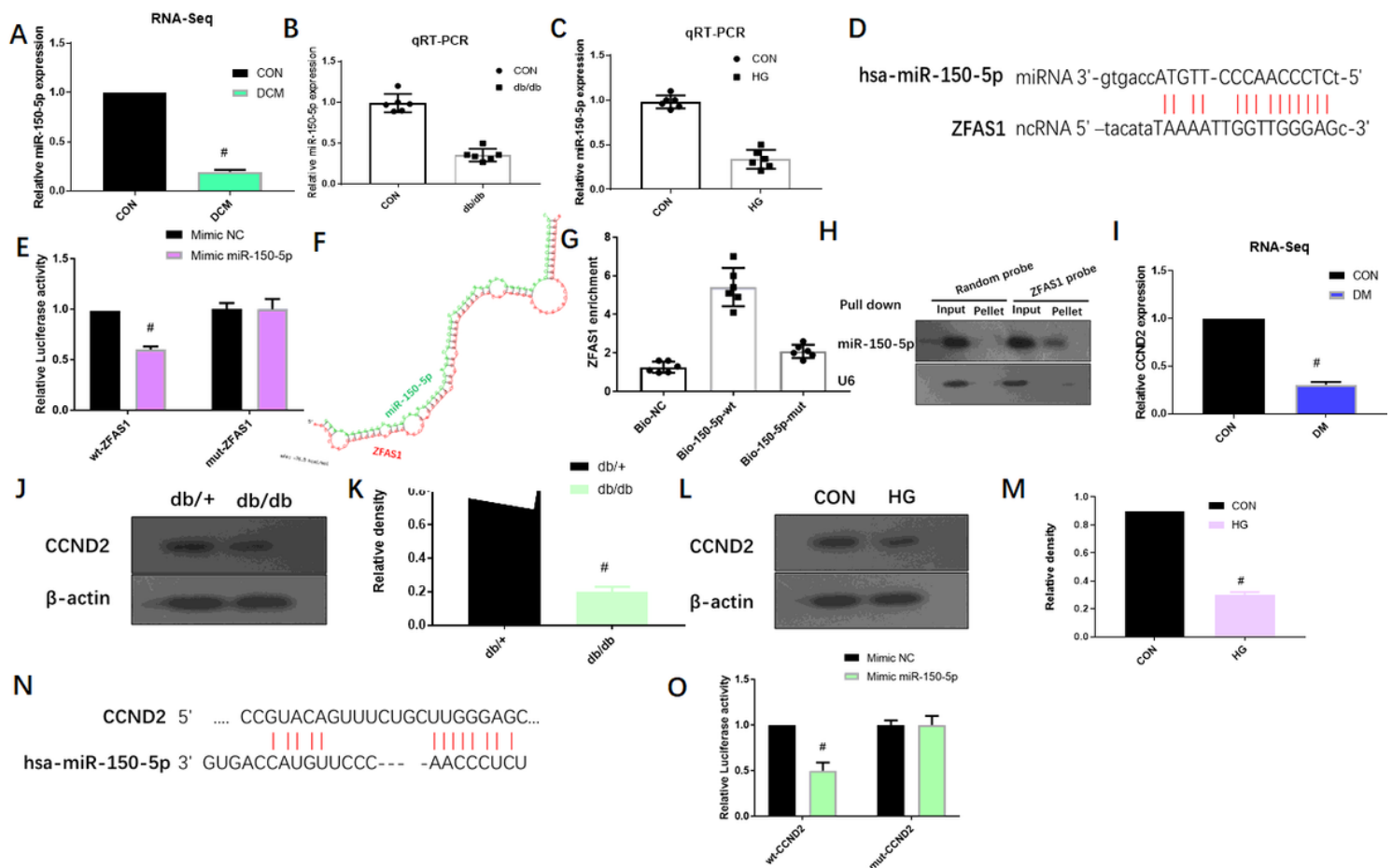


Figure 3

ZFAS1 can bind with miR-150-5p to regulate expression of CCND2. (A) MiR-150-5p expression levels in control group (CON) and diabetic cardiomyopathy (DCM) from RNA-sequencing data (GSE44179). (B) RT-qPCR analysis of miR-150-5p expression in the left ventricular myocardial tissues of db/+ and db/db mice. (C) RT-qPCR analysis of ZFAS1 expression in control cardiomyocytes and HG-treated cardiomyocytes. (D) The predicted bind site of miR-150-5p with ZFAS1 was analyzed by TargetScan program. (E) Dual luciferase reporter assay was used to confirm the binding of miR-150-5p with ZFAS1. (F) ZFAS1 contains a site complementary to miR-150-5p analyzed by RNAhybrid program. (G) miR-150-5p can bind directly to ZFAS1 in vivo performed by RNA Pull-down assay. (H) ZFAS1 can bind to miR-150-5p in vivo performed by RNA Pull-down assay. (I) CCND2 expression levels in the control rat ventricles and in the rat ventricles after STZ injection from RNA-sequencing data (GSE4745). (J-K) Relative protein expression of CCND2 by western blot analysis in the left ventricular myocardial tissues of db/+ and db/db mice. (L-M) Relative protein expression of CCND2 was assessed by western blot analysis in control cardiomyocytes and HG-treated cardiomyocytes. (N) The predicted bind site of CCND2 with ZFAS1 was analyzed by TargetScan program. (O) Dual luciferase reporter assay was used to confirm the binding of CCND2 with ZFAS1. #P < 0.05 vs CON group or db/+ group, data are measured as mean \pm SD (n=3).

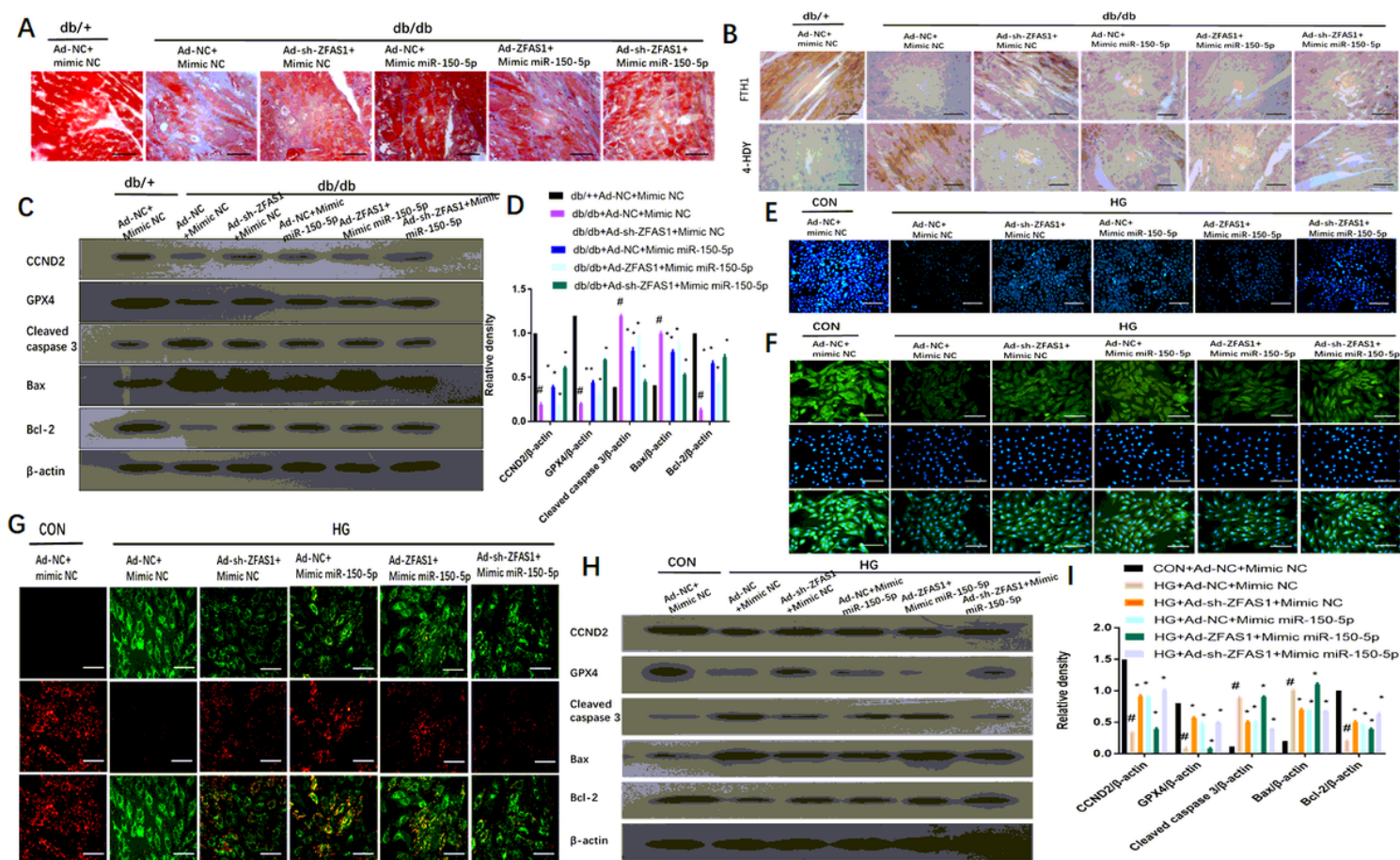


Figure 4

Inhibition of ZFAS1 repressed ferroptosis by up-regulating miR-150-5p in diabetic cardiomyopathy and HG-treated Cardiomyocytes. Db/+mice (n = 8) and db/db mice (n = 8) were injected with Ad-NC, Ad-ZFAS1, Ad-sh-ZFAS1, mimic NC, mimic miR-150-5p, respectively. Cardiomyocytes were transfected with Ad-NC, Ad-ZFAS1, Ad-sh-ZFAS1, mimic NC or mimic miR-150-5p with or without under HG stimulation. (A) Masson staining was used to assess collagen deposition in the left ventricular myocardial tissues in experimental mice (blue indicates collagen deposition). (B) Relative expression of FTH1 and 4-HNE were determined by immunohistochemical staining in the left ventricular myocardial tissues of experimental mice. (C-D) Relative protein expression of GPX4, Cleaved caspase 3, Bax, and Bcl-2 were assessed by western blot analysis in the left ventricular myocardial tissues of experimental mice. (E) MBB staining was used to assess GSH levels in experimental cardiomyocytes. (F) Immunofluorescence against FTH1 (green) in experimental cardiomyocytes. (G) JC-1 staining was used to assess mitochondrial membrane potential in experimental cardiomyocytes. (H-I) Relative protein expression of GPX4, Cleaved caspase 3, Bax, and Bcl-2 were assessed by western blot analysis in experimental cardiomyocytes. #P < 0.05 vs CON group +Ad-NC+mimic NC or db/+ +Ad-NC+mimic NC group, *P < 0.05 vs HG +Ad-NC+mimic NC or db/db +Ad-NC+mimic NC; data are measured as mean \pm SD (n=3).

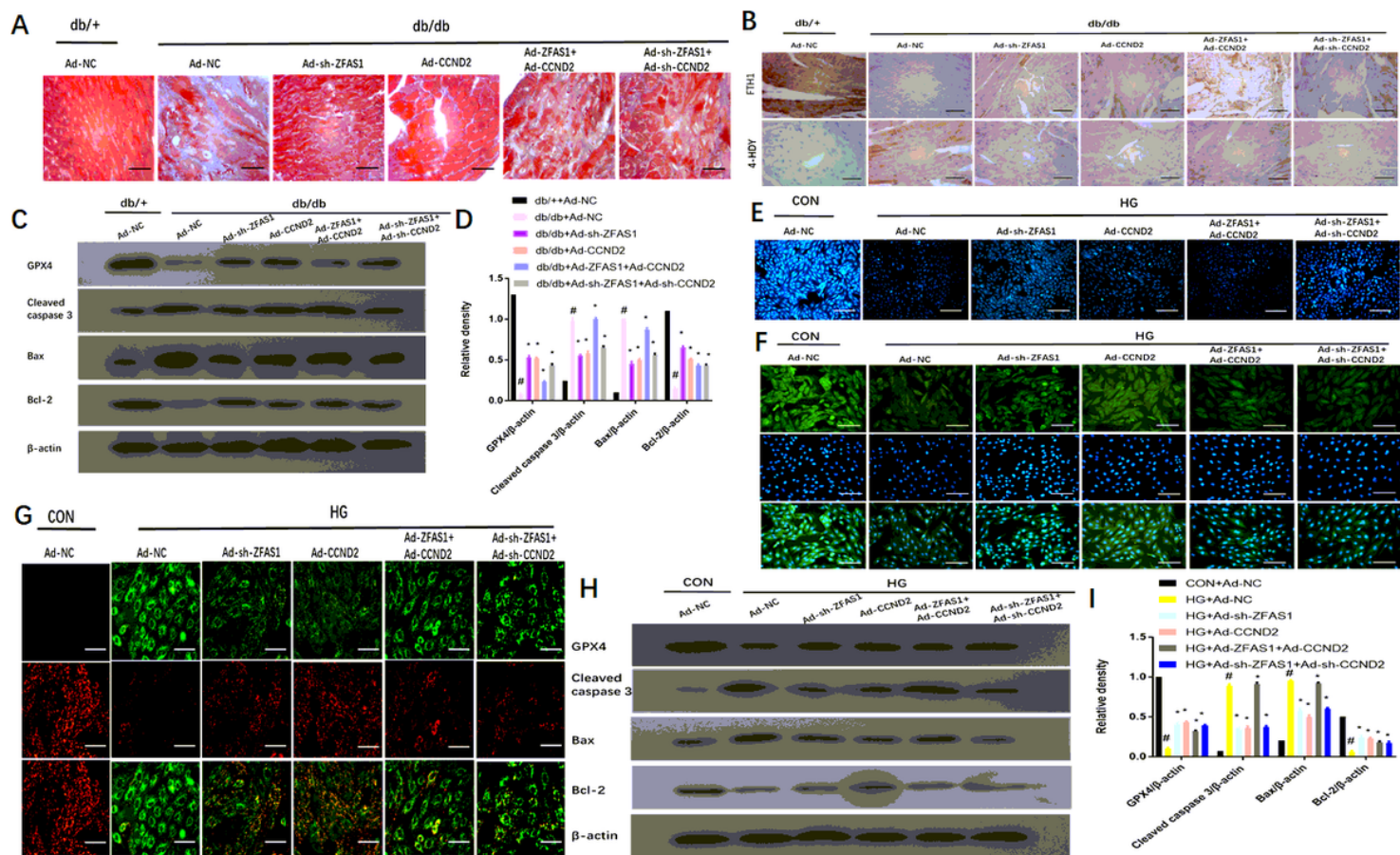


Figure 5

Inhibition of ZFAS1 alleviated ferroptosis by up-regulating CCND2 in diabetic cardiomyopathy and HG-treated Cardiomyocytes. Db/+mice (n = 8) and db/db mice (n = 8) were injected with Ad-NC, Ad-ZFAS1, Ad-sh-ZFAS1, Ad-CCND2, Ad-sh-CCND2, respectively. Cardiomyocytes were transfected with Ad-NC, Ad-ZFAS1, Ad-sh-ZFAS1, Ad-CCND2 or Ad-sh-CCND2 with or without under HG stimulation. (A) Masson staining was used to assess Collagen deposition in the left ventricular myocardial tissues in experimental mice (blue indicates collagen deposition). (B) Relative expression of FTH1 and 4-HNE were determined by immunohistochemical staining in the left ventricular myocardial tissues of experimental mice. (C-D) Relative protein expression of GPX4, Cleaved caspase 3, Bax, and Bcl-2 were assessed by western blot analysis in the left ventricular myocardial tissues of experimental mice. (E) MBB staining was used to assess GSH levels in experimental cardiomyocytes. (F) Immunofluorescence against FTH1 (green) in experimental cardiomyocytes. (G) JC-1 staining was used to assess mitochondrial membrane potential in experimental cardiomyocytes. (H-I) Relative protein expression of GPX4, Cleaved caspase 3, Bax, and Bcl-2 were assessed by western blot analysis in experimental cardiomyocytes. #P < 0.05 vs CON group +Ad-NC or db/+ +Ad-NC group, *P < 0.05 vs HG +Ad-NC or db/db + Ad-NC; data are measured as mean ± SD (n=3).

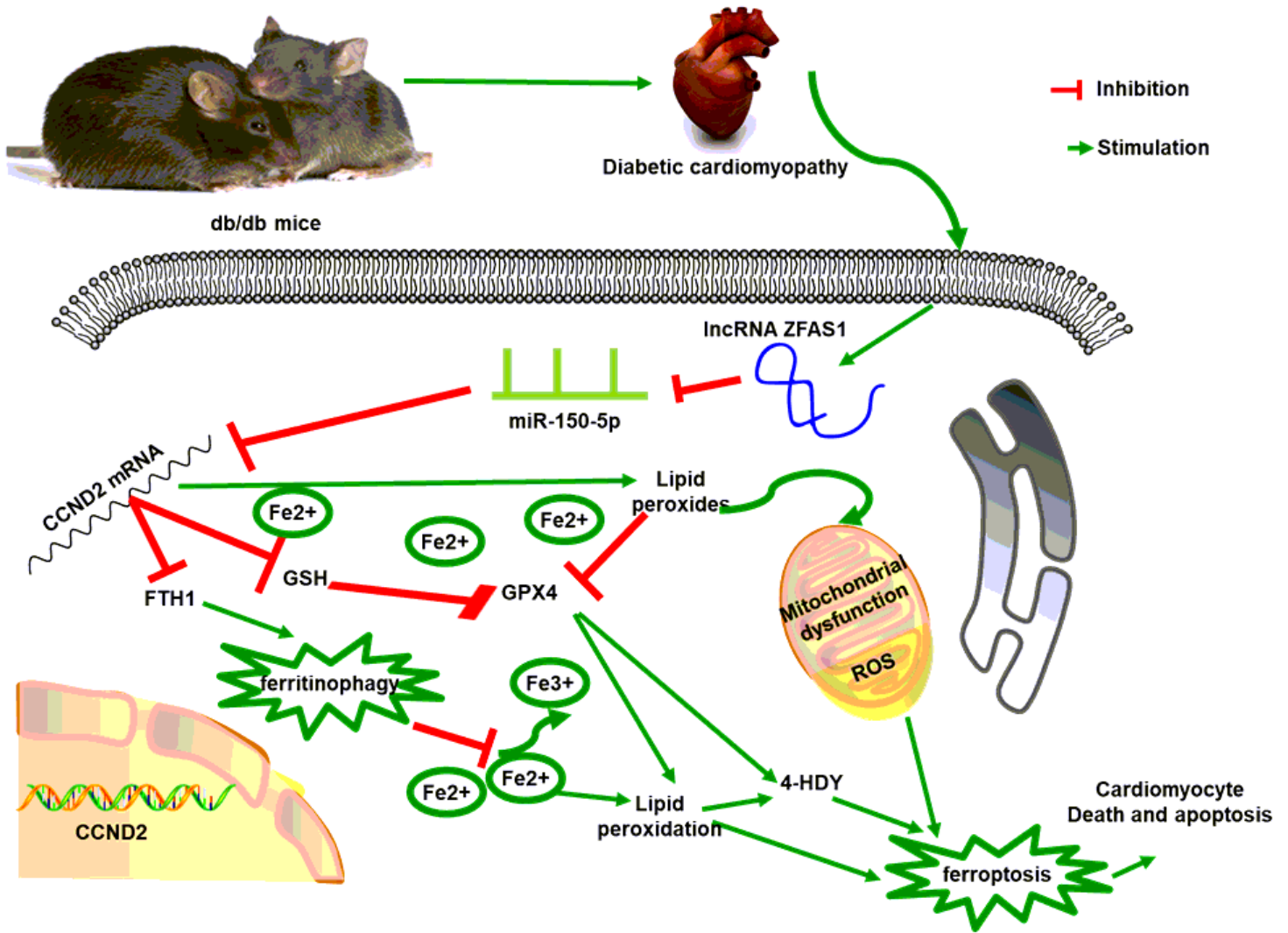


Figure 6

Schematic representing that ZFAS1 was highly expressed in DCM, ZFAS1 act as ceRNA to sponge miR-150-5p to regulate CCND2 expression, thereby indeed promote ferroptosis to accelerate diabetic cardiomyopathy.